Hindawi
Advances in Civil Engineering
Volume 2019, Article ID 9185756, 11 pages
https://doi.org/10.1155/2019/9185756

Research Article

Gaussian Process-Based Response Surface Method for Slope Reliability Analysis

Bin Hu,[1] Guo-shao Su,[2] Jianqing Jiang ,[2,3] and Yilong Xiao[2]

[1]*School of Resource and Environmental Engineering, Wuhan University of Science and Technology, P.O. Box 430081, Wuhan, China*
[2]*Key Laboratory of Disaster Prevention and Structural Safety of Ministry of Education, School of Civil and Architecture Engineering, Guangxi University, Nanning, Guangxi 530004, China*
[3]*Key Laboratory of Ministry of Education on Safe Mining of Deep Metal Mines, Northeastern University, Shenyang 110819, China*

Correspondence should be addressed to Jianqing Jiang; jiangqing880201@163.com

Received 25 November 2018; Revised 20 January 2019; Accepted 4 March 2019; Published 27 March 2019

Academic Editor: Eric Lui

A new response surface method (RSM) for slope reliability analysis was proposed based on Gaussian process (GP) machine learning technology. The method involves the approximation of limit state function by the trained GP model and estimation of failure probability using the first-order reliability method (FORM). A small amount of training samples were firstly built by the limited equilibrium method for training the GP model. Then, the implicit limit state function of slope was approximated by the trained GP model. Thus, the implicit limit state function and its derivatives for slope stability analysis were approximated by the GP model with the explicit formulation. Furthermore, an iterative algorithm was presented to improve the precision of approximation of the limit state function at the region near the design point which contributes significantly to the failure probability. Results of four case studies including one nonslope and three slope problems indicate that the proposed method is more efficient to achieve reasonable accuracy for slope reliability analysis than the traditional RSM.

1. Introduction

Slope stability analysis is an important issue in geotechnical engineering. The application of probabilistic concepts to the slope stability analysis has been pursued over the past decades. On real slope engineering, slope reliability can be obtained via an implicit limit state function with a numerical procedure employing the limit equilibrium methods [1, 2] or finite element method [3, 4]. The classical reliability analysis methods including first-order reliability method (FORM) and second-order reliability method (SORM) [5–8] that require limit state function gradients with respect to the basic variables may encounter great difficulties when direct or analytical differential is not possible. The Monte Carlo simulation (MCS) can handle the implicit performance function. However, the MCS was notorious for its unendurable computational cost.

The response surface method (RSM), which usually employs a polynomial function to approximate the unknown implicit performance function, has been used to the slope reliability analysis with the implicit performance function [4, 9–11]. However, the RSM is a rigidly nonadaptive regression technique in the statistical learning perspective [12]. Consequently, the RSM will become computationally impractical for problems involving many random variables, particularly when the involved random variables are mixed or statistically dependent. In addition, there is no guarantee that the fitted surface is a sufficiently close fit in all regions of interest.

In recent decades, machine learning methods such as artificial neural networks (ANN) [13–17], radial basis function network (RBFN) [18], and support vector machine (SVM) [19, 20] have been widely used for the reliability analysis. These methods can describe nonlinear and complex interactions among variables in a system and are therefore more suitable for solving reliability problems with highly nonlinear implicit performance. However, when

these machine learning methods are used, some difficulties will be encountered. For ANN, it is always difficult to obtain an appropriate network topology and the optimum hyperparameters. In addition, the ANN has some inherent drawbacks such as limitation in solving the small sample problem [21]. The SVM cannot avoid the blindness which is the common phenomenon in the artificial choice of the kernel function and its hyperparameter [21]. Hence, it is desirable to develop an efficient framework for slope reliability analysis.

The Gaussian process (GP), based on statistical learning theory and Bayesian theory, is a newly developed machine learning technology [22]. In recent years, the GP has gained considerable attention in the machine learning community and has been successfully applied in solving nonlinear, small samples, and high-dimensional problems [23–28]. The GP has many advantages, such as it does not require a predefined structure, can approximate arbitrary function landscapes including discontinuities and multimodality, has meaningful hyperparameters, and includes a theoretical framework for obtaining the optimum hyperparameter self-adaptively. Furthermore, GP provides an uncertainty measure in the form of a standard deviation for predicted function values.

In the present study, a new GP-based RSM for slope reliability analysis was put forward by combining the GP with the FORM. This paper is constructed as follows. The used machine learning technique, namely, Gaussian process regression, is briefly described in Section 2. The GP-based RSM method is presented in detail in Section 3. Finally, four case studies are used to verify the flexibility and efficiency of the proposed method.

2. Gaussian Process

A Gaussian process is a collection of random variables, any finite set of which has a joint Gaussian distribution. A Gaussian process can be defined by its mean function $m(\mathbf{x})$ and the covariance function $k(\mathbf{x}, \mathbf{x}')$ as

$$f(\mathbf{x}) \sim \mathrm{GP}\left(m(\mathbf{x}), k(\mathbf{x}, \mathbf{x}')\right). \tag{1}$$

There is a training set $\mathbf{D}$ of m observations, $\mathbf{D} = \{(\mathbf{x}_i, y_i) \mid i = 1, \ldots, m\}$, where $\mathbf{x}$ is an input vector with n dimensions and y is a scalar output or target. By using Bayesian forecasting, the distribution $p(y_* \mid \mathbf{x}_*, \mathbf{D})$ of output y_* given a test input $\mathbf{x}_*$ and a set of training points $\mathbf{D}$ can be calculated. Using the Bayesian rule, the posterior distribution for the Gaussian process outputs y_* can be obtained. By conditioning on the observed targets in the training set, the predictive distribution is Gaussian:

$$y_* \mid \mathbf{x}_*, \mathbf{X}, \mathbf{y} \sim N\left(\overline{y}(\mathbf{x}_*), \overline{\sigma}(\mathbf{x}_*)\right), \tag{2}$$

where the mean and variance are defined by

$$\overline{y}(\mathbf{x}_*) = \mathbf{k}_*^T\left(\mathbf{K} + \sigma_n^2\mathbf{I}\right)^{-1}\mathbf{y}, \tag{3}$$

$$\overline{\sigma}^2(\mathbf{x}_*) = k(\mathbf{x}_*, \mathbf{x}_*) - \mathbf{k}_*^T\left(\mathbf{K} + \sigma_n^2\mathbf{I}\right)^{-1}\mathbf{k}_*^T, \tag{4}$$

where the compact forms of the notation setting for the matrix of the covariance functions are $\mathbf{k}_* = \mathbf{K}(\mathbf{X}, \mathbf{x}_*)$, $\mathbf{K} = \mathbf{K}(\mathbf{X}, \mathbf{X})$, σ_n^2 is the unknown variance of the Gaussian noise.

Assuming $\boldsymbol{\alpha} = (\mathbf{K} + \sigma_n^2\mathbf{I})^{-1}\mathbf{y}$, equation (3) can be seen as a linear combination of m covariance functions, each one centered on a training point, by writing

$$\overline{y}(\mathbf{x}_*) = \sum_{j=1}^{m} \boldsymbol{\alpha}_j \mathbf{k}\left(\mathbf{x}_j, \mathbf{x}_*\right). \tag{5}$$

The Gaussian process procedure can handle interesting models by simply using a covariance function with an exponential term:

$$\mathbf{k}\left(\mathbf{x}_p, \mathbf{x}_q\right) = \sigma_f^2 \exp\left(-\frac{\left\|\mathbf{x}_p - \mathbf{x}_q\right\|^2}{2\mathbf{l}^2}\right) + \sigma_n^2\delta_{pq}, \tag{6}$$

where $\mathbf{l}$ denotes the characteristic length scale, σ_f^2 denotes the signal variance, and δ_{pq} denotes a Kronecker delta. This function expresses the idea the cases with nearby inputs will have highly correlated outputs. The GP employs a set of hyperparameters $\boldsymbol{\theta}$ including the length scale $\mathbf{l}$, the signal variance σ_f^2, and the noise variance σ_n^2. The hyperparameters $\boldsymbol{\theta}$ can be optimized based on the log-likelihood framework:

$$L = \log\, p(\mathbf{y} \mid \mathbf{X}, \boldsymbol{\theta}) = -\frac{1}{2}\mathbf{y}^T\mathbf{C}^{-1}\mathbf{y} - \frac{1}{2}\log\det\mathbf{C} - \frac{n}{2}\log 2\pi. \tag{7}$$

The log-likelihood and its derivative with respect to $\boldsymbol{\theta}$ can be described as

$$\frac{\partial L}{\partial \boldsymbol{\theta}} = -\frac{1}{2}tr\left(\mathbf{C}^{-1}\frac{\partial \mathbf{C}}{\partial \boldsymbol{\theta}}\right) + \frac{1}{2}\mathbf{y}^T\mathbf{C}^{-1}\frac{\partial \mathbf{C}}{\partial \boldsymbol{\theta}}\mathbf{C}^{-1}\mathbf{y}, \tag{8}$$

where $\mathbf{C} = \mathbf{K} + \sigma_n^2\mathbf{I}$.

Hyperparameters $\boldsymbol{\theta}$ are initialized to random values in a reasonable range and then optimized using an iterative, such as the conjugate gradient.

More detailed theory of the GP can be found in the literature [24].

3. GP-Based RSM

3.1. Explicit Formation of Reliability Index Using GP. The performance function of a slope can be built as follows:

$$g(\mathbf{X}) = F_s - 1, \tag{9}$$

where $\mathbf{X}$ denotes the random variables with mean $\boldsymbol{\mu}_\mathbf{x}$ and standard deviation $\boldsymbol{\sigma}_\mathbf{x}$. $g(\mathbf{X}) > 0$ indicates a stable slope, while $g(\mathbf{X}) < 0$ indicates a failed slope. $g(\mathbf{X}) = 0$ indicates that the slope is hovering between stable and unstable. F_s is the safety factor.

Assuming that there is a point $\mathbf{x}^* = (x_1^*, x_2^*, \ldots, x_n^*)^T$ located on the limit state surface, which is called as the design point. Here, n is the dimension of $\mathbf{x}^*$. $g(\mathbf{x})$ is generally a nonlinear function. However, it can be linearized at $\mathbf{x}^*$ by neglecting the second- or upper-order term:

$$Z_Q = g(\mathbf{x}^*) + \sum_{i=1}^{n} \frac{\partial g(\mathbf{x}^*)}{\partial x_i} (x_i - x_i^*). \tag{10}$$

Assuming $\mathbf{x}$ is statistically uncorrelated, the mean value and standard deviation of Z_Q are defined by

$$\mu_{Z_Q} = g(\mathbf{x}^*) + \sum_{i=1}^{n} \frac{\partial g(\mathbf{x}^*)}{\partial x_i} \left(\mu_{x_i} - x_i^*\right),$$
$$\sigma_{Z_Q} = \sqrt{\sum_{i=1}^{n} \left[\frac{\partial g(\mathbf{x}^*)}{\partial x_i}\right]^2 \sigma_{x_i}^2}. \tag{11}$$

Reliability index can be calculated by

$$\beta = \frac{\mu_{Z_Q}}{\sigma_{Z_Q}} = \frac{g(\mathbf{x}^*) + \sum_{i=1}^{n} \left(\partial g(\mathbf{x}^*)/\partial x_i\right)\left(\mu_{x_i} - x_i^*\right)}{\sqrt{\sum_{i=1}^{n} \left[\partial g(\mathbf{x}^*)/\partial x_i\right]^2 \sigma_{x_i}^2}}. \tag{12}$$

According to the FORM, a tangent hyperplane is used to fit the limit state surface at the design point. Therefore, the most important step in the method is to obtain the design point. Reliability index β is defined as the distance from the origin to the design point. Hence, the coordinate of the design point $\mathbf{x}^*$ is denoted as

$$x_i^* = \mu_{x_i} + \beta \sigma_{x_i} \cos\, \theta_{x_i}, \quad i = 1, 2, \ldots, n, \tag{13}$$

where

$$\cos \theta_{x_i} = -\frac{\left(\partial g(\mathbf{x}^*)/\partial x_i\right)\sigma_{x_i}}{\sqrt{\sum_{i=1}^{n} \left[\partial g(\mathbf{x}^*)/\partial x_i\right]^2 \sigma_{x_i}^2}}. \tag{14}$$

According to equation (5), the performance function can be approximated by the GP model as

$$g(\mathbf{x}^*) \approx \overline{y}(\mathbf{x}^*) = \sum_{j=1}^{m} \boldsymbol{\alpha}_j \mathbf{k}\left(\mathbf{x}_j, \mathbf{x}^*\right). \tag{15}$$

The first-order partial derivatives of the approximate function can be given by

$$\frac{\partial g(\mathbf{x}^*)}{\partial x_i} \approx \frac{\partial \overline{y}(\mathbf{x}^*)}{\partial x_i} = \sum_{j=1}^{m} \boldsymbol{\alpha}_j \frac{\partial \mathbf{k}\left(\mathbf{x}_j, \mathbf{x}^*\right)}{\partial x_i}, \tag{16}$$

where $\left(\partial \mathbf{k}(\mathbf{x}_j, \mathbf{x}^*)/\partial x_i\right) = (x_i^* - x_{ij}/l_i^2)\sigma_f^2 \exp\left(-(1/2\mathbf{l}^2)\right.$ $\left.\cdot \|\mathbf{x}_j - \mathbf{x}^*\|^2\right)$.

Substituting equations (15) and (16) into (17), the reliability index β is given as

$$\beta = \frac{\sum_{j=1}^{m} \boldsymbol{\alpha}_j \mathbf{k}\left(\mathbf{x}_j, \mathbf{x}^*\right) + \mu_y + \sum_{i=1}^{n}\sum_{j=1}^{m} \boldsymbol{\alpha}_j \left(\partial \mathbf{k}\left(\mathbf{x}_j, \mathbf{x}^*\right)/\partial x_i\right)\left(\mu_{x_i} - x_i^*\right)}{\sqrt{\sum_{i=1}^{n}\sum_{j=1}^{m} \left[\boldsymbol{\alpha}_j \left(\partial \mathbf{k}\left(\mathbf{x}_j, \mathbf{x}^*\right)/\partial x_i\right)\right]^2 \sigma_{x_i}^2}}. \tag{17}$$

According to equations (15) and (16), (14) can be rewritten as

$$\cos \theta_{x_i} = -\frac{\sum_{j=1}^{m} \boldsymbol{\alpha}_j \left(\partial \mathbf{k}\left(\mathbf{x}_j, \mathbf{x}^*\right)/\partial x_i\right)\sigma_{x_i}}{\sqrt{\sum_{i=1}^{n} \left[\sum_{j=1}^{m} \boldsymbol{\alpha}_j \left(\partial \mathbf{k}\left(\mathbf{x}_j, \mathbf{x}^*\right)/\partial x_i\right)\right]^2 \sigma_{x_i}^2}}. \tag{18}$$

Substituting equations (17) and (18) into (13), one can obtain the coordinate of design point $\mathbf{x}^*$ using GP approximation.

The failure probability can be calculated as

$$p_f \approx \Phi(-\beta), \tag{19}$$

where $\Phi(\cdot)$ denotes the cumulative distribution function of the standard normal variable.

3.2. Procedure of GP-Based RSM. The main difference between the GP-based RSM and the traditional RSM is that the former employs the GP to approximate the performance function and its first-order partial derivatives simultaneously. Moreover, from the viewpoint of machine learning theory, more knowledge means a better effect on the result of training or prediction of the machine learning model. Thus, the training samples, namely, knowledge set in the machine learning domain, is generated as a dynamic updating one to improve the performance of the GP model in the procedure of GP-based RSM.

As shown in Figure 1, reliability analysis using the GP-based RSM is described in detail as follows:

Step 1. Assume initial values of the design point $\mathbf{x}^* = (x_1, x_2, \ldots, x_n)$. Usually, mean values of the random variables can be selected as the coordinates of the design point $\mathbf{x}^*$.

Step 2. According to the experimental plan of the RSM developed by Bucher and Bourgund [29]; the training samples are generated according to the intersection of the axis $\mathbf{x}(\mu_1, \mu_2, \ldots, \mu_n)$ and coordinates of $x_i = \mu_i$ and $\mu_i \pm f\sigma_i$, where μ_i and σ_i are the mean and standard deviation of the random variable x_i. f, which is an integer, ranges from 1 to 4 and is usually set to 1. Then, values of the performance function $y(x_1, x_2, \ldots, x_n)$ containing $y(\mu_1, \mu_2, \ldots, \mu_i \pm f\sigma_i, \ldots, \sigma_n)$ and $y(\mu_1, \mu_2, \ldots, \sigma_n)$ are obtained using the slope analysis code. Thus, the training samples $\mathbf{D} = (\mathbf{x}_i, y_i)$ are established, and the number of training samples is $2n \times s + 1$. s is the number of selected f.

Step 3. If the training target $\mathbf{y}$ has a nonzero mean, to improve the efficiency of the training process of the model, $\mathbf{y}$ is adjusted by the mean μ_y of $\mathbf{y}$

$$\widehat{y}_i = y_i - \mu_y. \tag{20}$$

Step 4. Train the GP model by learning the training samples $\mathbf{D} = \{(\mathbf{x}_i, \widehat{y}_i) \mid i = 1, \ldots, m\}$. Then, we make predictions of performance function on the design point $\mathbf{x}^*$ and obtain their predictions $\overline{y}(x^*)$ according to equation (5). Recall that the training targets were centered, thus we must adjust the predictions by offset:

$$g(\mathbf{x}^*) \approx \overline{y}(\mathbf{x}^*) + \mu_y = \sum_{j=1}^{m} \boldsymbol{\alpha} \mathbf{k}\left(\mathbf{x}_j, \mathbf{x}^*\right) + \mu_y. \tag{21}$$

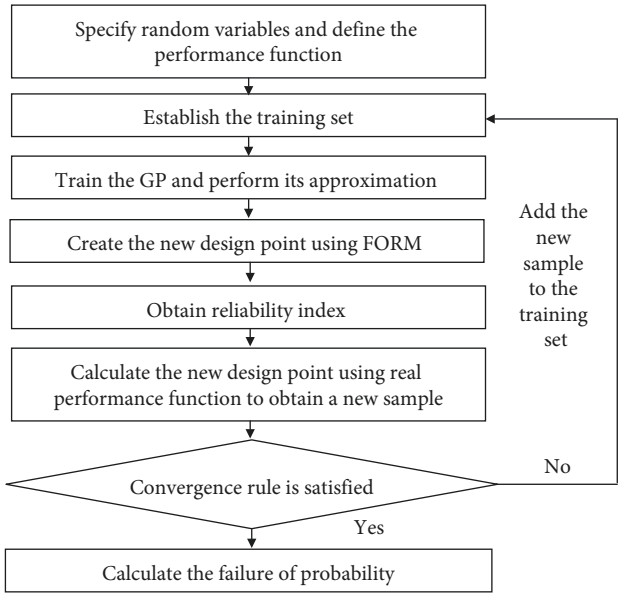

Figure 1: Flow chart of the GP-based RSM.

Step 5. Compute the reliability index of the k^{th} iteration step $\beta^{(k)}$ using equation (17).

Step 6. Compute the values of the new design point according to equation (21).

Step 7. Check the convergence criterion for $\left|\beta^{(k)} - \beta^{(k-1)}\right| \le \varepsilon$ (ε is 0.001 in present paper). To improve constantly the reconstructing precision at the important region where the failure probability is contributed significantly, the new design point and its value of the real performance function are taken as a new sample added into the old training sample if the convergence criteria are not satisfied. The number of training samples increases to $2n \times s + 1 + k$. Go to step 3 and repeat steps 3–6 until convergence is satisfied. If the convergence criterion is satisfied, go to step 8.

Step 8. Calculate the probability of failure p_f using equation (19).

To apply the GP-Based RSM to slope reliability analysis, a general program package is developed using **MATLAB**.

4. Case Studies

4.1. Case 1: A Highly Nonlinear Performance Function. The performance function of the first example is defined as [30]

$$g(x_1, x_2) = 2 + \exp\left(-\frac{x_1^2}{10}\right) + \left(\frac{x_1}{5}\right)^4 - x_2, \tag{22}$$

where x_1 and x_2 are independent and obey standard normal distribution with zero mean and unit standard deviation.

The training samples and predicted values of the performance function are listed in Table 1. There are 5 training samples generated using the proposed method, where f is 1. The optimum hyperparameters of trained GP $\boldsymbol{\theta} = (3.5197,$ 5.4426, 4.8151, −9.6465). The small prediction error from the GP indicates that the training is successful. If a vector of the basic random variables is input, the GP can generate an adequate accurate value of the corresponding performance function. Consequently, the GP can represent the true performance function well.

Table 1: Training samples and the predicted values using GP for Example 1.

No.	x_1	x_2	$g(x)$	GP approximation
1	−1	0	2.9064	2.9064
2	0	−1	4.0000	4.0000
3	1	0	2.9064	2.9063
4	0	1	2.0000	2.0000
5	0	0	3.0000	2.9999

The GP approximation of the performance function based on the initial training samples is

$$g(x_i) \approx \sum_{j=1}^{m} \boldsymbol{\alpha}_i \mathbf{k}\left(\mathbf{x}_i, \mathbf{x}_j\right) + 2.9625, \tag{23}$$

where the covariance function $k(x_i, x_j)$ denotes the column of matrix $\mathbf{K}$ and the values of vector $\boldsymbol{\alpha}$ and matrix $\mathbf{K}$ based on the initial training samples are as follows:

$$\boldsymbol{\alpha} = \begin{bmatrix} -7.8560 & 1.8422 & -7.8568 & -1.7191 & 14.7597 \end{bmatrix},$$

$$\mathbf{K} = \begin{bmatrix} 0.9524 & 0.7190 & 0.7535 & 0.7190 & 0.8983 \\ & 0.9524 & 0.7190 & 0.3909 & 0.7623 \\ & & 0.9524 & 0.7190 & 0.8983 \\ & \text{sym.} & & 0.9524 & 0.7623 \\ & & & & 0.9542 \end{bmatrix}. \tag{24}$$

Table 2 lists both calculation processes of the design point using the FORM and the proposed method. It clearly illustrates that the real performance and its first derivatives are both fitted very well by the GP model.

The failure probability and reliability index obtained by various methods in preexisting studies are listed in Table 3. The exact reliability index is 2.9044 obtained by the direct MCS [30]. The reliability index yielded by the FORM, RSM, and GP-based RSM are very close to that by the MCS. The GP-based RSM needs 7 function evaluations, while the RSM and direct MCS require 19 and 10^6 function evaluations, respectively.

Figure 2 shows the curves of approximated limit state function from the GP based on final training samples composed of 5 initial samples and 2 new samples and that of real limit state function. As can be seen from Figure 3, the GP can capture the whole shape of the real limit state function, and the design point is found quickly by the use of the GP-based RSM. This shows that the dynamic update of the training samples can significantly improve the efficiency of searching the design point in the proposed method.

Table 2: Calculation process of the design point using FORM and the proposed method for Example 1.

Method	Iterations	Design point		First derivative		Reliability index
		x_1^*	x_2^*	$(\partial g/\partial x_1^*)$	$(\partial g/\partial x_2^*)$	β
FORM	I	0	0	0	−1	3
	II	0	3	0	−1	3
	III	0	3	—	—	3
GP-based RSM	I	0	0	0.0000	−1.0875	2.7026
	II	0.0000	2.7026	−0.0001	−0.9999	3.0000
	III	0.0002	3.0000	−0.0052	−0.9999	3.0000
	IV	0.0157	3.0000	—	—	3.0000

Table 3: Results of Example 1 using different methods.

Method	MCS	FORM	RSM	GP-based RSM
Reliability index	2.9040	3.0000	3.0000	3.0000
Probability of failure ($\times 10^{-3}$)	1.8420	1.3498	1.3500	1.3498
Number of function evaluation	10^6	2	19	7

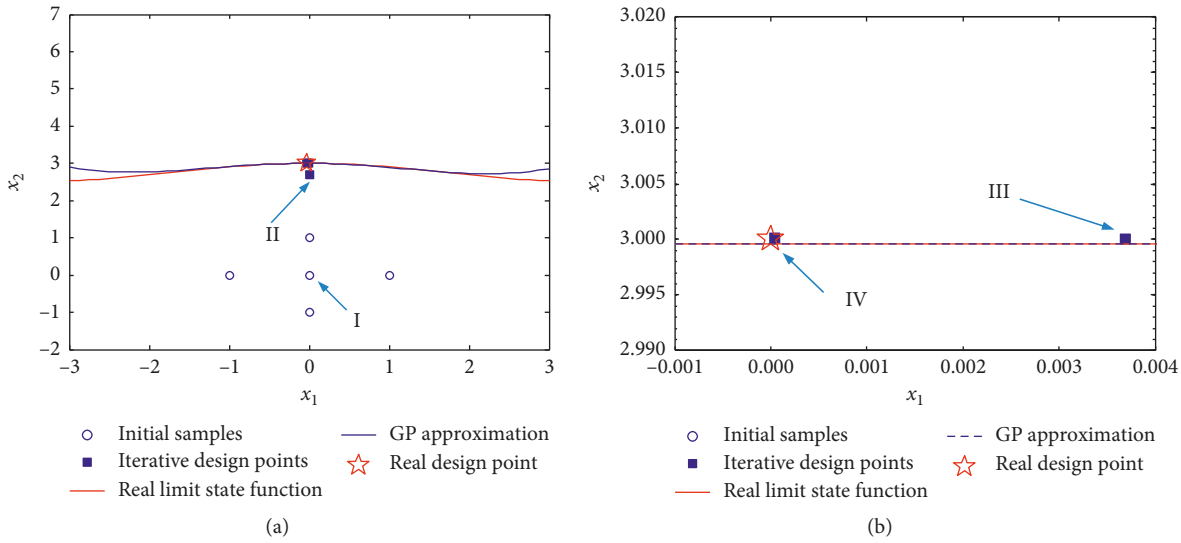

Figure 2: Compare the curve of limit state function from GP based on the final training samples with that from the real limit state function, where the boxes refer to the design points at iterative step in GP-based RSM: (b) enlarged figure; (a) in the range of $-0.001 \le x_1 \le 0.004$, $2.990 \le x_2 \le 3.020$.

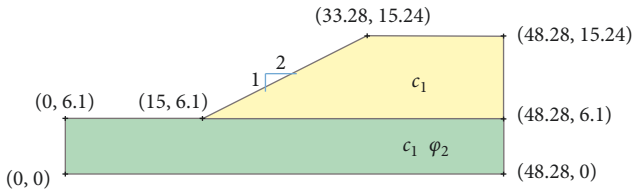

Figure 3: Geometry of slope for Example 2.

4.2. Case 2: A Two-Layered Slope. As illustrated in Figure 3, the second example considers a two-layered slope which has been studied by Xu and Low [4]; Cho [14]; Hassan and Wolff [31]; Bhattacharya et al. [32]; and Chowdhury and Rao [33]. Property parameters of the soil related to the slope, including the friction angle and cohesion, are taken as random variables, as listed in Table 4. These random variables are assumed to obey normal distribution variables in the numerical analysis. Unit weight of the soil is assumed to be 19 kN/m^3. By numerical analysis using SLIDE [24], the factor of safety $F(\mathbf{x})$ of circular slip surface was calculated using the Bishop and Spencer methods, respectively.

There are 7 training samples ($f = 1$) established for training the GP model as shown in Table 5. The safety factors of the other 10 samples created randomly were predicted using the trained GP model. The safety factors calculated by the Bishop code and Spencer method and values predicted by the GP are shown in Figure 4. The GP model can reflect the relationship between the random variables and the safety factor of the slope. Then, the performance functions in the explicit form using the GP model were established to approximate the implicit real performance functions.

Table 4: Properties of stochastic variables of Example 2.

Random variable	Mean	Standard deviation
c_1 (kN/m^2)	38.31	7.662
c_2 (kN/m^2)	23.94	4.788
φ_2 (deg)	12	1.2

Table 5: The initial learning samples of Example 2.

Sample nos.	c_1 (kN/m^2)	c_2 (kN/m^2)	φ_2 (deg)	$g(x)$		GP approximation	
				Bishop	Spencer	Bishop	Spencer
1	30.648	23.94	12	0.4576	0.4596	0.4576	0.4596
2	38.31	19.152	12	0.5412	0.5506	0.5412	0.5506
3	38.31	23.94	10.8	0.6047	0.6133	0.6051	0.6133
4	45.972	23.94	12	0.7795	0.7857	0.7795	0.7857
5	38.31	28.728	12	0.7442	0.7622	0.7442	0.7622
6	38.31	23.94	13.2	0.6792	0.6955	0.6796	0.6954
7	38.31	23.94	12	0.6443	0.6564	0.6433	0.6564

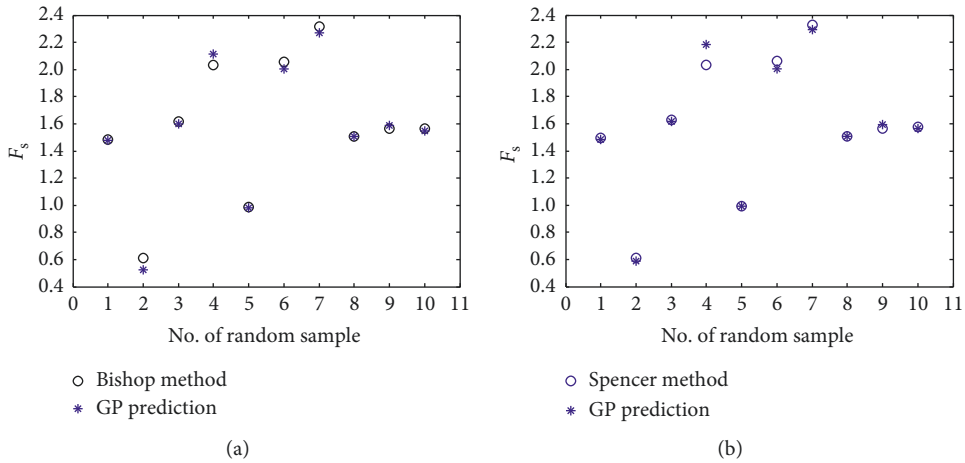

Figure 4: Comparison between safety factors calculated by (a) Bishop method and GP prediction and (b) Spencer method and GP prediction.

Table 6 listed the results of the probabilistic analyses obtained from the previous literature for the same problem, while Tables 7 and 8 present the results obtained by the GP-based RSM. It can be observed from Tables 7 and 8, the result of reliability index by the early study shows that the exact solution is about 2.2 [33], and the reliability index estimation by the GP-based RSM with 7 initial samples is 2.249 from the Bishop method and 2.269 from the Spencer method, respectively. The results are quite in agreement with each other.

Furthermore, Tables 7 and 8 indicate that the change of the numbers of initial training samples slightly influences the accuracy of estimated values of probability of failure. It is worth noting that a larger number of initial training samples may mean higher robust and computation cost of the proposed method at the same time. The proposed method needs 12 function evaluations, while the ANN [14], MCS, first-order HDMR-based response surface method, and second-order HDMR-based response surface method [33] requires 25, 10^6, 13, and 61 number of original stability analysis, respectively. The larger the number of the function evaluations, the more the time needed to finish the computation is, the less efficient the used method is. Consequently, the GP-based RSM method is relatively efficient.

The slip surfaces from the Bishop method and Spencer method at the mean point and at the design point are shown in Figures 5 and 6, respectively. The slip surfaces at the mean point are very different from that at the design point. The values of the factor of safety F_s at the design point are both very close to 1; in another words, $g(\mathbf{X}) \approx 0$, which mean the slope just reaches the limited equilibrium status.

4.3. Case 3: A Three-Layered Slope. A complex slope with three different soil layers is studied. The cross section of the nonhomogeneous slope with a height of 10 m and an inclination of 2 : 1 is presented in Figure 7. The unit weight

Table 6: Results of probabilistic analysis from different methods for Example 2.

Method	Reliability index	Failure probability
Hassan and Wolff [31]: MVFOSM, Spencer method, noncircular slip surface	2.869	—
Bhattacharya et al. [32]: MVFOSM, Spencer method, noncircular slip surface by direct search	2.861	—
Crum [34]	2.23	1.29×10^{-2}
Xu and Low [4]: response surface method, FEM	2.18	1.46×10^{-2}
Xu and Low [4]: spreadsheet-based direct implementation of Spencer's method with the search for the critical slip surface	2.20	1.39×10^{-2}
Cho [14]: ANN-based response surface method with FORM	2.189	1.43×10^{-2}
Chowdhury and Rao [33]: direct Monte Carlo (1×10^6 samples) using the Bishop method, circular slip surface	2.203	1.38×10^{-2}
Chowdhury and Rao [33]: second-order HDMR, Bishop method	2.228	1.29×10^{-2}
Chowdhury and Rao [33]: second-order HDMR, Spencer method	2.198	1.39×10^{-2}
GP-based RSM ($f=1$): Bishop method	2.249	1.23×10^{-2}
GP-based RSM ($f=1$): Spencer method	2.269	1.16×10^{-2}

Table 7: Results of probabilistic analysis by the Bishop method for Example 2.

Number of initial training samples	7 ($f=1$)	13 ($f=1$, 2)	19 ($f=1$, 2, 3)	25 ($f=1$, 2, 3, 4)
Reliability index	2.249	2.251	2.253	2.251
Design point				
c_1 (kN/m^2)	21.198	21.070	21.055	21.074
c_2 (kN/m^2)	24.374	23.784	23.908	23.852
φ_2 (deg)	11.701	12.080	12.073	12.097
F_s of design point	1.008	1.002	1.001	1.002

Table 8: Results of probabilistic analysis by the Spencer method for Example 2.

Number of initial training samples	7 ($f=1$)	13 ($f=1$, 2)	19 ($f=1$, 2, 3)	25 ($f=1$, 2, 3, 4)
Reliability index	2.269	2.265	2.253	2.251
Design point				
c_1 (kN/m^2)	20.962	20.958	21.093	21.116
c_2 (kN/m^2)	24.318	23.790	23.861	23.845
φ_2 (deg)	11.852	12.007	12.199	12.208
F_s of design point	1.001	1.001	1.007	1.008

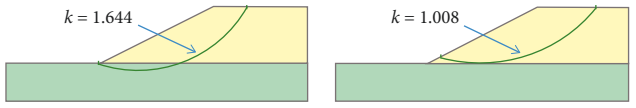

Figure 5: Example 2: results of the stability analysis by the Bishop method. Slip surface at (a) the mean point ($F_s=1.644$) and (b) the design point ($F_s=1.008$).

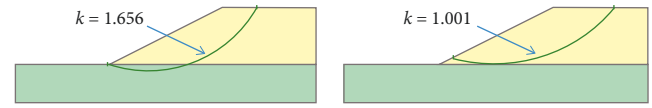

Figure 6: Example 2: results of the stability analysis by the Spencer method. Slip surface at (a) the mean point ($F_s=1.656$) and (b) the design point ($F_s=1.001$).

$\gamma=19.5\,\text{kN}\cdot\text{m}^{-3}$. The corresponding property parameters of the soil related to the slope, including the cohesion c and friction angle φ, are considered as random variables. These random variables obey the normal distribution. The values of the mean and standard deviation of the random variables are listed in Table 9.

The calculations of the safety factor of the slope are conducted using the Bishop method and the Spencer method by the SLIDE code [35]. 11 initial training samples ($f=1$) are listed in Table 10 while the safety factor of the circular slip surface was calculated using the Bishop and Spencer methods, respectively.

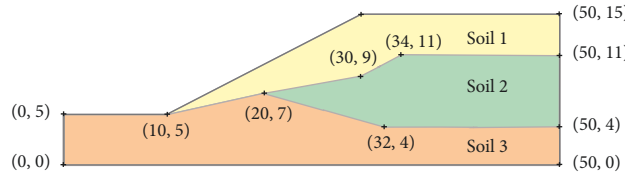

Figure 7: Geometry of the slope of Example 3.

Table 9: Properties of stochastic variables of Example 3.

Soil type	c (kPa)		φ (deg)	
	Mean value	Standard deviation	Mean value	Standard deviation
1	0	0	38	4
2	5.3	0.7	23	3
3	7.2	0.2	20	3

Table 10: The initial learning samples of Example 3.

Sample nos.	φ_1 (deg)	c_2 (kN/m^2)	φ_2 (deg)	c_3 (kN/m^2)	φ_3 (deg)	$g(x)$	
						Bishop	Spencer
1	38	5.3	23	7.2	20	0.4052	0.3747
2	34	5.3	23	7.2	20	0.3493	0.3251
3	38	4.6	23	7.2	20	0.4009	0.3705
4	38	5.3	20	7.2	20	0.3744	0.3491
5	38	5.3	23	7	20	0.3994	0.3691
6	38	5.3	23	7.2	17	0.3009	0.2685
7	42	5.3	23	7.2	20	0.4507	0.4192
8	38	6	23	7.2	20	0.4096	0.3788
9	38	5.3	26	7.2	20	0.4343	0.4008
10	38	5.3	23	7.4	20	0.4111	0.3803
11	38	5.3	23	7.2	23	0.5033	0.4757

Table 11: Results comparison of Example 3.

Method	SLIDE [35] MCS (1×10^6 samples)		SVM-based RSM [20]		GP-based RSM	
	Bishop	Spencer	Bishop	Spencer	Bishop	Spencer
Reliability index β	3.542	3.287	3.4293	3.0481	3.4853	3.2118
Number of function evaluation	10^6	10^6	19	19	12	12

The results of the slope reliability analysis using different methods are listed in Table 11. A sampling size of 10^6 is considered in the direct MCS by numerical analysis using SLIDE [35] to estimate the failure probability P_f. The failure probability estimation by the GP-based RSM is in good agreement with that of the MCS. The proposed method needs 12 function evaluations, while the number of function evaluations for the SVM-based RSM [20] and MCS are 19 and 10^6, respectively. This indicates that the proposed GP-based RSM is much more efficient to achieve reasonable accuracy for slope reliability analysis than the SVM-based RSM [20].

In addition, the slip surfaces from the Bishop method and Spencer method at the design point obtained using the proposed method are both presented in Figure 8.

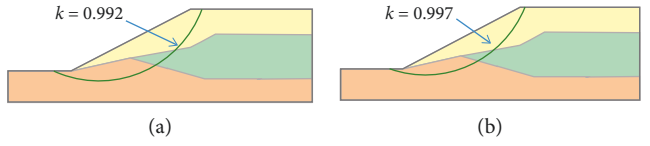

Figure 8: Example 3: results of the stability analysis. Slip surface at the design point by (a) the Bishop method ($F_s = 0.992$) and (b) the Spencer method ($F_s = 0.997$).

4.4. Example 4: Congress St. Cut Model. In this example, the confessed Congress St. Cut model studied by Chowdhury and Xu [36] is considered. The soil profile is presented in Figure 9. Two sets of circular slip surfaces are considered. The first set consists of potential failure surface tangential to the lower boundary of the Clay 2 layer (failure mode I), while the second considers slip surfaces tangential to the lower boundary of Clay 3 (failure mode II). The property parameters of soil are listed in Table 12 and are assumed to obey the Gaussian distribution in the numerical analysis. The Bishop method is used to estimate the safety factor from the

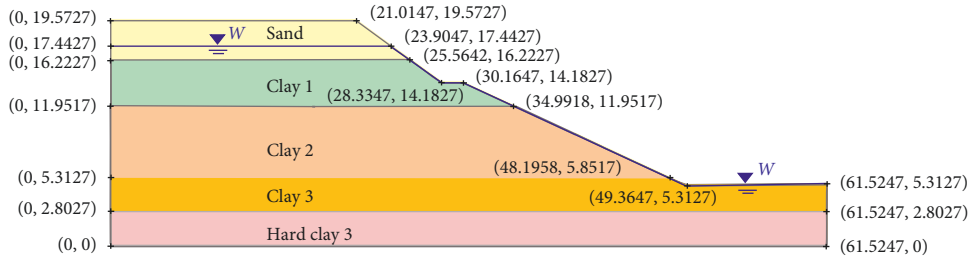

Figure 9: Geometry of slope of Example 4.

Table 12: Material properties of the soil of Example 4.

Material	c (kPa)		φ (deg)		r (kN/m^3)
	Mean	Standard deviation	Mean	Standard deviation	
Clay 1	68.1	6.6	0	—	21
Clay 2	39.3	1.4	0	—	22
Clay 3	50.8	1.5	0	—	22
Sand	0	—	0	—	21
Hard clay	200	—	35	—	—

Table 13: The initial learning samples of Example 4.

Sample nos.	c_1 (kN/m^2)	c_2 (kN/m^2)	c_3 (kN/m^2)	$g(x)$	
				Failure mode I	Failure mode II
1	68.1	39.3	50.8	0.1083	0.0578
2	61.5	39.3	50.8	0.0798	0.0398
3	68.1	37.9	50.8	0.0793	0.0505
4	68.1	39.3	49.3	0.1083	0.0382
5	74.7	39.3	50.8	0.1368	0.0758
6	68.1	40.7	50.8	0.1373	0.0652
7	68.1	39.3	52.3	0.1083	0.0775

Table 14: Results of probabilistic analyses using different methods for Example 4.

Method	Failure mode	Probability of failure
Chowdhury and Rao [33]: direct Monte Carlo (5000 samples) using the Bishop method, circular slip surface	I	0.0037
	II	0.0175
Chowdhury and Rao [33]: first-order HDMR, Bishop method	I	0.0041
	II	0.0171
Chowdhury and Rao [33]: second-order HDMR, Bishop method	I	0.0044
	II	0.0166
Chowdhury and Xu [36]	I	0.0048
	II	0.0131
GP-based RSM: Bishop method	I	0.0039
	II	0.0185

numerical analysis using SLIDE [35]. For evaluating the failure probability P_f, $f=1$ is selected, which results in 7 initial training samples (Table 13). Without any iteration, totally 7 actual stability analyses using the Bishop method are needed for the GP-based RSM. It can be observed from Table 14 that the failure probability estimated by the GP-based RSM agrees well with that reported in the literature [33]. However, the total numbers of slope stability analysis for the proposed method is 12, while that for the MCS, first-order HDMR, and second-order HDMR are 5000, 13, and 61, respectively [33] This indicates that the proposed method is very efficient to achieve reasonable accuracy. The slip surface of failure mode I and failure mode II at the design point obtained using the proposed method are both presented in Figure 10.

5. Conclusions

A GP-based RSM was developed to predict failure probability of slope. In this method, the training samples for

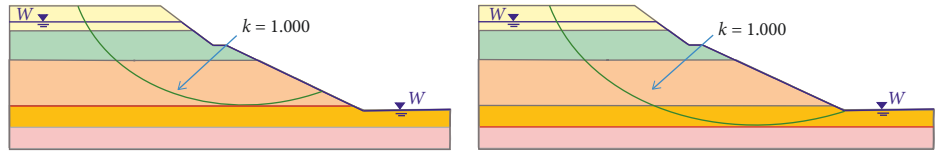

Figure 10: Example 4: results of the stability analysis by Bishop method. Slip surface at the design point: (a) failure model I, $F_s = 1.000$ and (b) failure model II, $F_s = 1.000$.

establishing the GP model are first generated by the design method of the classical RSM method. The limit state function and its first-order partial derivative are then approximated by the trained GP model. Finally, failure probability is estimated using the FORM. In addition, the viewpoint of more knowledge means the better effect on the result of training or prediction of the machine learning model, and the use of the renewed continuously training samples may improve the performance of the GP model for approximating the limit state function around the design point. Thus, the GP significantly reduces the number of required training samples. Otherwise, GP also shows good performance to approximate the limit state function and then provides accurate estimation of the failure probability when connected with the FORM. Four numerical examples including both slope and nonslope problems illustrate the flexibility and efficiency of the proposed method. Compared with the traditional RSM, the GP-based RSM is much more efficient to achieve reasonable accuracy for slope reliability analysis. Moreover, the present method can directly take advantage of existing slope software without modification and thus are convenient to be used for practitioner engineers. However, it should be noted that the proposed algorithm is intended as a possible complement rather than a replacement for existing classical methods.

Data Availability

The data used to support the findings of this study are included within the article.

Conflicts of Interest

The authors declare that they have no conflicts of interest.

Acknowledgments

This study was financially supported by the National Natural Science Foundation of China under Grant no. 51369007.

References

[1] A. W. Bishop, "The use of the slip circle in the stability analysis of slopes," *Géotechnique*, vol. 5, no. 1, pp. 7–17, 1955.

[2] E. Spencer, "A method of analysis of the stability of embankments assuming parallel inter-slice forces," *Géotechnique*, vol. 17, no. 1, pp. 11–26, 1967.

[3] T. Matsui and K.-C. San, "Finite element slope stability analysis by shear strength reduction technique," *Soils and Foundations*, vol. 32, no. 1, pp. 59–70, 1992.

[4] B. Xu and B. K. Low, "Probabilistic stability analyses of embankments based on finite-element method," *Journal of Geotechnical and Geoenvironmental Engineering*, vol. 132, no. 11, pp. 1444–1454, 2006.

[5] E. E. Alonso, "Risk analysis of slopes and its application to slopes in Canadian sensitive clays," *Géotechnique*, vol. 26, no. 3, pp. 453–472, 1977.

[6] C. A. Cornell, "First-order uncertainty analysis of soil deformation and stability," in *Proceedings of the 1st International Conference on Application of Probability and Statistics in Soil and Structural Engineering (ICAPI)*, pp. 129–144, Hong Kong, China, February 1972.

[7] K. S. Li and P. Lumb, "Probabilistic design of slopes," *Canadian Geotechnical Journal*, vol. 24, no. 4, pp. 520–535, 1987.

[8] A. I. H. Malkawi, W. F. Hassan, and F. A. Abdulla, "Uncertainty and reliability analysis applied to slope stability," *Structural Safety*, vol. 22, no. 2, pp. 161–187, 2000.

[9] J. T. Christian, C. C. Ladd, and G. B. Baecher, "Reliability applied to slope stability analysis," *Journal of Geotechnical Engineering*, vol. 120, no. 12, pp. 2180–2207, 1994.

[10] D. V. Griffiths and G. A. Fenton, "Probabilistic slope stability analysis by finite elements," *Journal of Geotechnical and Geoenvironmental Engineering*, vol. 130, no. 5, pp. 507–518, 2004.

[11] F. S. Wong, "Slope reliability and response surface method," *Journal of Geotechnical Engineering*, vol. 111, no. 1, pp. 32–53, 1985.

[12] J. E. Hurtado, "An examination of methods for approximating implicit limit state functions from the viewpoint of statistical learning theory," *Structural Safety*, vol. 26, no. 3, pp. 271–293, 2004.

[13] K. W. Chau, "Reliability and performance-based design by artificial neural network," *Advances in Engineering Software*, vol. 38, no. 3, pp. 145–149, 2007.

[14] S. E. Cho, "Probabilistic stability analyses of slopes using the ANN-based response surface," *Computers and Geotechnics*, vol. 36, no. 5, pp. 787–797, 2009.

[15] J. Deng, D. Gu, X. Li, and Z. Q. Yue, "Structural reliability analysis for implicit performance functions using artificial neural network," *Structural Safety*, vol. 27, no. 1, pp. 25–48, 2005.

[16] A. H. Elhewy, E. Mesbahi, and Y. Pu, "Reliability analysis of structures using neural network method," *Probabilistic Engineering Mechanics*, vol. 21, no. 1, pp. 44–53, 2006.

[17] J. E. Hurtado and D. A. Alvarez, "Neural-network-based reliability analysis: a comparative study," *Computer Methods in Applied Mechanics and Engineering*, vol. 191, no. 1-2, pp. 113–132, 2001.

[18] J. Deng, "Structural reliability analysis for implicit performance function using radial basis function network," *International Journal of Solids and Structures*, vol. 43, no. 11-12, pp. 3255–3291, 2006.

[19] A. Basudhar, S. Missoum, and A. Harrison Sanchez, "Limit state function identification using Support Vector Machines

for discontinuous responses and disjoint failure domains," *Probabilistic Engineering Mechanics*, vol. 23, no. 1, pp. 1–11, 2008.

[20] H.-b. Zhao, "Slope reliability analysis using a support vector machine," *Computers and Geotechnics*, vol. 35, no. 3, pp. 459–467, 2008.

[21] V. N. Vapnik, *The Nature of Statistical Learning Theory*, Springer, Berlin, Germany, 1995.

[22] D. J. C. MacKay, "Introduction to Gaussian processes," Technical Report, Cavendish Laboratory, Cambridge University, Cambridge, UK, 1998.

[23] J. Hensman, R. Mills, S. G. Pierce, K. Worden, and M. Eaton, "Locating acoustic emission sources in complex structures using Gaussian processes," *Mechanical Systems and Signal Processing*, vol. 24, no. 1, pp. 211–223, 2010.

[24] C. E. Rasmusen and C. K. I. Williams, *Gaussian Processes for Machine Learning*, The MIT Press, Cambridge, MA, USA, 2006.

[25] G. Su, J. Jiang, B. Yu, and Y. Xiao, "A Gaussian process-based response surface method for structural reliability analysis," *Structural Engineering and Mechanics*, vol. 56, no. 4, pp. 549–567, 2015.

[26] G. Xiao, L. Peng, and L. Hu, "A Gaussian process-based dynamic surrogate model for complex engineering structural reliability analysis," *Structural Safety*, vol. 68, pp. 97–109, 2017.

[27] G. S. Su, L. B. Yan, and Y. C. Song, "Gaussian process for nonlinear displacement time series prediction of landslide," *Journal of China University of Geosciences*, vol. 18, no. 1, pp. 219–221, 2007.

[28] C. K. I. Williams, "Prediction with Gaussian processes: from linear regression to linear prediction and beyond," in *Proceedings of the Nato Advanced Study Institute on Learning in Graphical Models*, pp. 599–621, Kluwer Academic Publishers, Norwell, MA, USA, March 1998.

[29] C. G. Bucher and U. Bourgund, "A fast and efficient response surface approach for structural reliability problems," *Structural Safety*, vol. 7, no. 1, pp. 57–66, 1990.

[30] Z. Guo and G. Bai, "Application of least squares support vector machine for regression to reliability analysis," *Chinese Journal of Aeronautics*, vol. 22, no. 2, pp. 160–166, 2009.

[31] A. M. Hassan and T. F. Wolff, "Search algorithm for minimum reliability index of earth slopes," *Journal of Geotechnical and Geoenvironmental Engineering*, vol. 125, no. 4, pp. 301–308, 1999.

[32] G. Bhattacharya, D. Jana, S. Ojha, and S. Chakraborty, "Direct search for minimum reliability index of earth slopes," *Computers and Geotechnics*, vol. 30, no. 6, pp. 455–462, 2003.

[33] R. Chowdhury and B. N. Rao, "Probabilistic stability assessment of slopes using high dimensional model representation," *Computers and Geotechnics*, vol. 37, no. 7-8, pp. 876–884, 2010.

[34] K. S. Li and R. W. M. Cheung, "Discussion of "search algorithm for minimum reliability index of earth slopes" by K. S. Li and raymond W. M. Cheung," *Journal of Geotechnical and Geoenvironmental Engineering*, vol. 127, no. 2, pp. 197–205, 2001.

[35] Rocscience Inc., *Slide 2D limit equilibrium slope stability for soil and rock slopes:Verification Manual*, Rocscience Inc., Toronto, ON, Canada, 2006.

[36] R. N. Chowdhury and D. W. Xu, "Geotechnical system reliability of slopes," *Reliability Engineering & System Safety*, vol. 47, no. 3, pp. 141–151, 1995.